The Stability Analysis of Slopes with a Slip Surface of General Shape

Analyse de la stabilité des pentes à surface de glissement de forme générale

E. NONVEILLER, DR.SC.TECH., *Professor of Soil Mechanics, University of Zagreb, Yugoslavia*

SUMMARY

Several solutions exist for the practical computation of the safety factor of slopes on circular slip surfaces. For slip surfaces of general shape, graphical solutions and Janbu's numerical solution (limited to elongated shallow slip surfaces) are available. An expression is derived for the numerical computation of the safety factor, which satisfies all conditions of equilibrium and which is applicable to slip surfaces of any shape. It is shown that the results obtained are accurate. The advantage of the proposed expression is that it can be programmed for digital computers.

SOMMAIRE

Il y a plusieurs solutions pour le calcul pratique du coefficient de sécurité des pentes aux surfaces de glissement circulaires. Pour les surfaces de glissement de forme générale, on dispose de solutions graphiques et de la solution numérique de Janbu, laquelle est limitée aux surfaces de glissement oblongues et peu profondes. On a dérivé une formule permettant de calculer le coefficient de sécurité satisfaisant toutes les conditions d'équilibre et applicable aux surfaces de glissement de forme quelconque. L'auteur démontre que les résultats obtenus sont exacts. L'avantage de la formule proposée réside dans son application dans les calculs au moyen de calculateurs électroniques.

THE SLIP SURFACE OF SLOPES IN HOMOGENEOUS SOILS can be approximated very closely to a circular cylinder. The safety factor is expressed as the ratio of the available shearing strength of the material and the tangential stresses needed for equilibrium thus:

$$F_s = \tau_f/\tau,$$

$$\tau = c'/F_s + \sigma'(\tan\phi'/F_s). \qquad (1)$$

Various methods for the computation of the safety factor (F_s), either graphical (Krey, 1936; Taylor, 1948) or numerical (Bishop, 1955) have been elaborated with some simplifying assumptions on the distribution of normal stresses along the slip circle and the plastic equilibrium has been attained along the whole slip surface.

The shape of the slip surface may differ considerably from the circular arc if the material of the slope is not homogeneous, the difference increasing with the importance of the variation of the shearing strength along the potential slip surface. The slip surface in stratified material may be shallow and elongated or deep with sharp breaks as shown on Figs. 1 and 5. It may even be convex as shown analytically by Samsioe (1955) and Trollope (1957) as well as experimentally by Nonveiller (1953, 1955, 1957) and Reinius (1961). In such cases the stability analysis is carried out graphically (Reinius, 1955; Nonveiller, 1957) or numerically (Janbu, 1954).

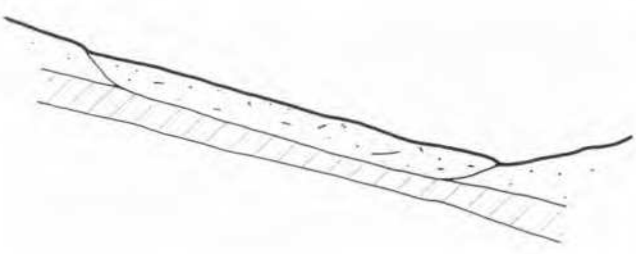

FIG. 1. Slip surface of general shape.

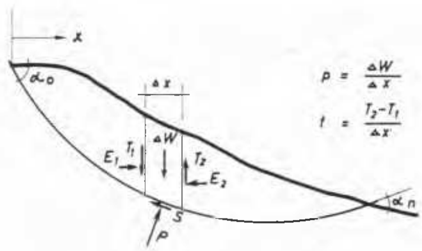

$$F_s = \frac{\Sigma\,(c' + (p+t-u)\tan\phi')\left[\dfrac{\Delta x}{\cos^2\alpha\,(1+\tan\phi'\tan\alpha/F_s)}\right]}{\Sigma\,(p+t)\,\Delta x\,\tan\alpha}$$

$$= \frac{\Sigma\,(c' + (p+t-u)\tan\phi')\Delta x\left[\dfrac{1}{\cos\alpha\,(1+\frac{\tan\phi'\tan\alpha}{F_s})}\cdot\dfrac{1}{\cos\alpha}\right]}{\Sigma\,(p+t)\,\Delta x\,\sin\alpha\,\frac{1}{\cos\alpha}} = \frac{\Sigma A\cdot\frac{1}{\cos\alpha}}{\Sigma B\cdot\frac{1}{\cos\alpha}} \quad \ldots\ldots (2)$$

$$F_s = \frac{\Sigma\,(c' + (p+t-u)\tan\phi')\cdot\Delta x\left[\dfrac{1}{\cos\alpha\,(1+\frac{\tan\phi'\tan\alpha}{F_s})}\right]}{\Sigma\,(p+t)\,\Delta x\,\sin\alpha} = \frac{\Sigma A}{\Sigma B} \quad \ldots\ldots (3)$$

$R = \infty$, $\cos\alpha = const$ $(1) \equiv (2)$

$R < \infty$, $\cos\alpha = f(x)$ $(1) \neq (2)$

FIG. 2. Janbu and Bishop equations (2 and 3 respectively) for factor of safety.

Janbu's numerical solution can be applied to elongated shallow slip surfaces, but is seriously in error when applied to deep slip surfaces. Janbu's solution considers only the momentum equilibrium of every single slice, but for the whole sliding segment it remains unbalanced. As shown on Fig. 2 Janbu's Equation 2 applied to a circular slip surface does not yield the same result as Bishop's Equation 3, as it should were the solution correct and applicable to any shape of the slip surface. The results of Equations 2 and 3 applied to the same circular arc differ from each other the more the difference between the angles α_0 and α_n increases. The results would be identical for a plane slip surface, which can be regarded as part of a circular arc with $R = \infty$.

In order to obtain an equation for the computation of the safety factor which is valid for sliding surfaces of any shape the condition of the momentum equilibrium of the whole sliding mass above the slip surface must be satisfied.

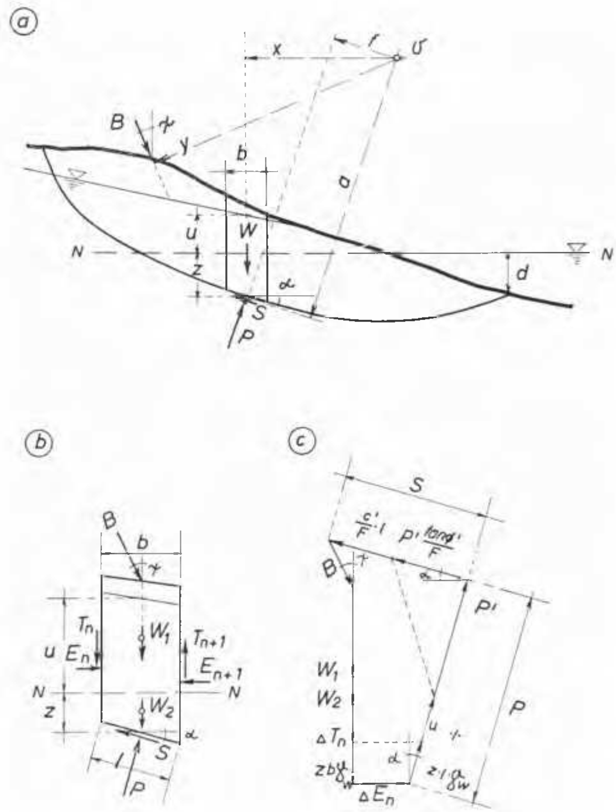

FIG. 3. (a) Sliding segment with forces and levers; (b) forces on slice n; (c) polygon of forces on slice n.

Fig. 3 shows such a sliding segment with a slip surface of varying radius, with the relative force levers acting on slice n around pole 0, in an arbitrary position. We denote: c', ϕ' the shear strength parameters along the slip surface; u, the excess pore pressure on the slip surface; σ_n, the normal stress on the slip surface; τ, the shear stress on the slip surface; P, the total normal force acting on the slip surface through a slice; S, the shear force acting on the slip surface through a slice.

In accordance with Fig. 3 we have

$$\sigma_n = P/l, \tag{4}$$

and substituting in Eq. 1 we obtain the shear stress mobilized to satisfy the condition of limiting equilibrium:

$$\tau = (1/F_s)[c' + (P/l - u) \tan \phi']. \tag{5}$$

The shear force acting on a slice is $S = \tau . l$, and equating the moment of the active forces (W,B) with the moment of the resisting forces (P,S) we obtain

$$\sum (Wx + By) = (1/F_s) \sum [c'l + (P - ul) \tan \phi'] \cdot a + \sum P \cdot f + \frac{1}{2} d^2 a_1. \tag{6}$$

Resolving for F_s we obtain with Eqs 4 and 5:

$$F_s = \frac{\sum [c'l + (P - ul) \tan \phi'] a}{\sum (Wx + By) - \sum P \cdot f - \frac{1}{2} d^2 a_1} \tag{7}$$

in which W is the total weight of soil and water, P is the total normal force acting on any slice, and (a_1) is the lever of the hydrostatic pressure on the vertical section at the lower end of the slip surface. Since the water below the line N-N is in equilibrium, the statically equivalent disturbing moment of the weight is obtained as $\Sigma(W_1 + W_2).x$ and the moment of the resulting component of the total normal force as $P_1 f$, in which $P_1 = P - \gamma_w . z . 1 = P' + u . 1$. Eq 7 can now be written as:

$$F_s = \frac{\sum [c'l + P' \tan \phi'] \cdot a}{\sum [(W_1 + W_2)x + By] - P_1 \cdot f}. \tag{7a}$$

The polygon of forces acting on slice n is shown on Fig. 3 (c) in a general case, when the sliding segment is partially submerged and pore pressure appears in part of the slope. From the polygon of forces we get by resolving vertically:

$$B \cos \psi + W_1 + W_2 + \Delta T + bz\gamma_w = lz\gamma_w \cos \alpha + (P' + ul) \cos \alpha + (1/F_s) [c'l + P' \tan \phi'] \sin \alpha. \tag{8}$$

W_1 denotes the full weight of soil above water level N-N (unit weight γ); W_2 denotes the submerged weight of soil below water level N-N (unit weight γ'); γ_w denotes unit weight of water.

From Eq 8 we get the effective normal force on slice n

$$P' = \frac{B \cos \psi + W_1 + W_2 + \Delta T - ub - \frac{c}{F_s} b \tan \alpha}{\cos \alpha \left(1 + \frac{\tan \phi' \tan \alpha}{F_s}\right)}, \tag{9}$$

and the component of the total normal force on slice n

$$P_1 = P + ul = \left[B \cos \psi + W_1 + W_2 + \Delta T + (ub \tan \phi' - c'b) \frac{\tan \alpha}{F_s}\right] \Big/ \cos \alpha \left(1 + \frac{\tan \phi' \tan \alpha}{F_s}\right). \tag{10}$$

Introducing P_1 and P' from Eqs 9 and 10 into Eq 7a we get an implicit equation for the computation of the safety factor:

$$F_s = \left(\sum [c'b + (B \cos \psi + W_1 + W_2 + \Delta T - ub) \times \tan \phi'] \frac{a}{m\alpha}\right) \Big/ \left(\sum [By + (W_1 + W_2)x] - \sum \left[B \cos \psi + W_1 + W_2 + \Delta T + (ub \tan \phi' - c'b) \frac{\tan \alpha}{F_s}\right] \cdot \frac{f}{m\alpha}\right) \tag{11}$$

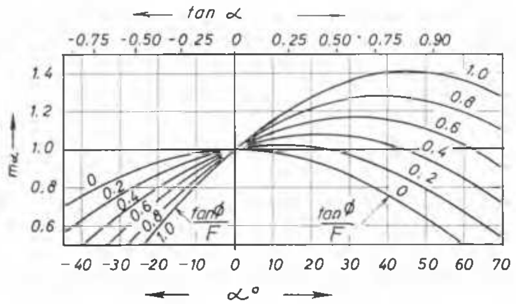

FIG. 4. Chart for (m_α) values in Equations 2, 3, and 9 (Janbu, Bjerrum, Kjaernsli).

in which $m = \cos\alpha\,[1 + (\tan\phi' \tan\alpha/F_s)]$. For easy application the factor (m_α) can be obtained from the diagram on Fig. 4.

Eq 11 will reduce to Bishop's equation 3 if applied to a circular slip surface with the pole 0 in the centre of the circle.

The normal components E and the tangential components T of the forces acting on the vertical sections between the slices must satisfy the following conditions:

$$\sum \Delta T = 0,$$

$$\sum \Delta E = -\gamma_w (d^2/2). \qquad (12)$$

Computing ΔE from the resolution of forces on a slice in the direction of the tangential force S we obtain from Fig. 3b:

$$S = (B \sin\psi + \Delta E)\cos\alpha + (B\cos\psi + W_1 + W_2 + \Delta T + bz\gamma_w)\sin\alpha$$

and

$$\Delta E = S\sec\alpha + B[\sin(\alpha+\psi)/\cos\alpha] - (W_1 + W_2 + \Delta T)\tan\alpha - bz\gamma_w \tan\alpha. \qquad (13)$$

Introducing in accordance with Eqs 5, 6, and 11

$$S = (1/F_s)[c'b + (B\cos\psi + W_1 + W_2 + \Delta T - ub) \times \tan\phi'](1/m_\alpha) = [m]/F_s,$$

Eq 13 becomes

$$\sum(\Delta E + bz\gamma_w \tan\alpha) = \sum\left[\frac{[m]}{F_s}\sec\alpha - B\frac{\sin(\alpha+\psi)}{\cos\alpha} - (W_1 + W_2 + \Delta T)\tan\alpha\right] \qquad (13a)$$

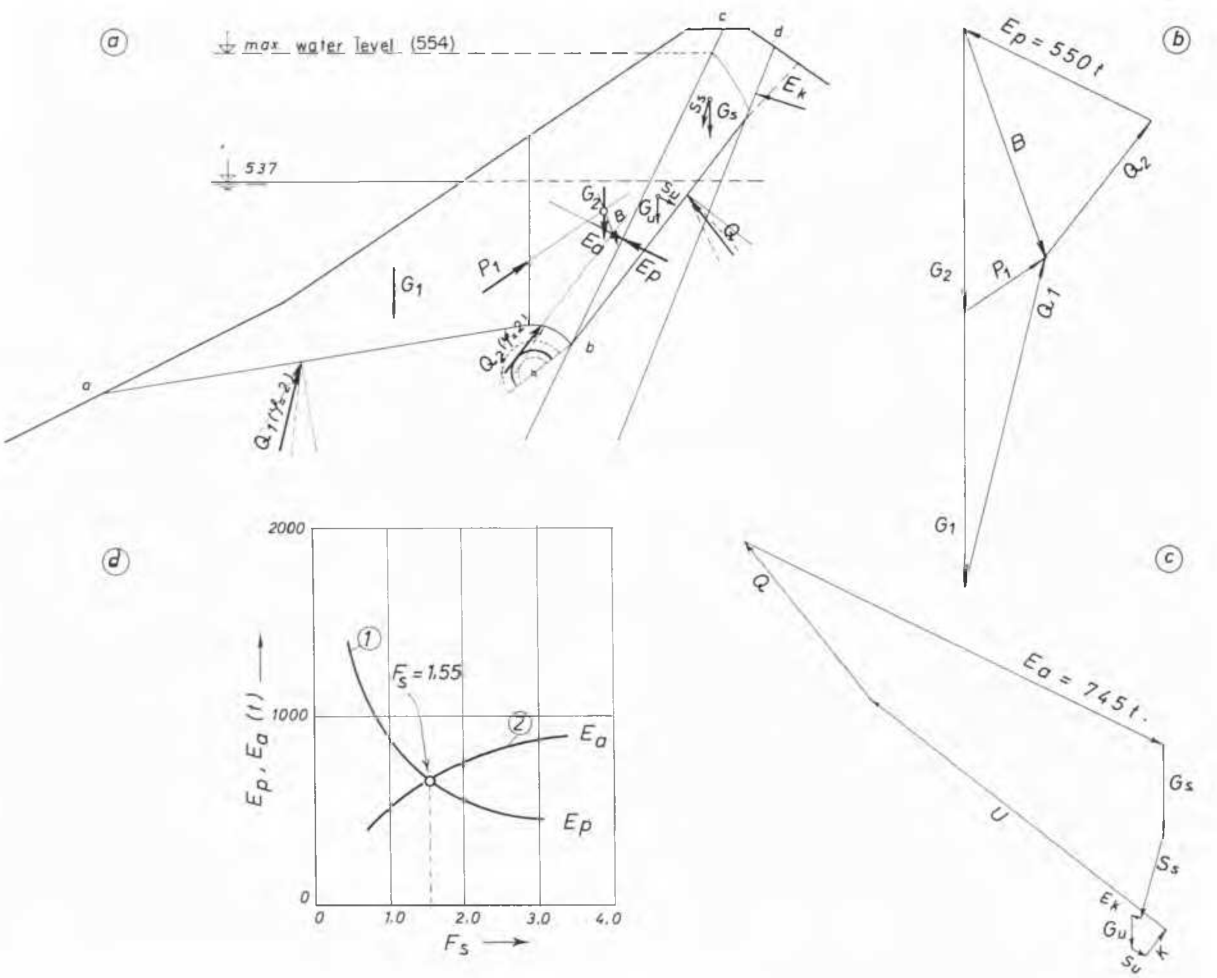

FIG. 5. Graphical solution of factor of safety, upstream slope of rockfill dam, sudden drawdown from maximum water level 554 to water level 537: (a) forces on segment and slip surface; (b) polygon of forces on passive wedge (a b c) for $F_s = 2.0$; (c) polygon of forces on active wedge (b c d) for $F_s = 2.0$; (d) interpolation of factor of safety for $E_a = E_p$, (1) resistance (E_p) of passive wedge (a b c) for various F_s, (2) pressure (E_a) of active wedge (b c d) for various F_s, (3) Eq 11, $\Delta T = 0$, $F_s = 1.60$, Eqs 11 and 14, $F_s = 1.55$.

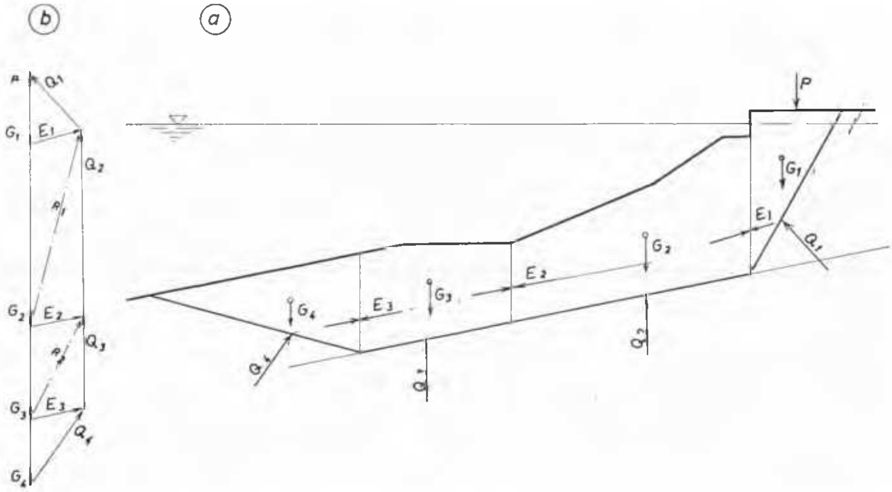

FIG. 6. (a) Slip surface and sliding wedge; (b) polygon of forces for $F_s = 1.80$. Results: Graphically $F_s = 1.80$; Eq 11 with $T = 0$, $F_s = 1.85$; Eqs 11 and 14 $F_s = 1.78$; Eq 1 $F_s = 1.38$.

Since $\Sigma bz\gamma_w \tan \alpha = \gamma_w(d^2/2)$ it follows from Eq 13a that $\Sigma\Delta E + \Sigma bz\gamma_w \tan \alpha \equiv 0$, from which we get the second condition which the forces ΔT must satisfy:

$$\sum\left[\frac{[m]}{F_s}\sec\alpha - B\frac{\sin(\alpha+\psi)}{\cos\alpha} - (W_1 + W_2 + \Delta T)\tan\alpha\right] = 0. \quad (14)$$

In many cases it can be assumed that $T = E = 0$ without prohibitive loss of accuracy as seen in the example cited below. A more comprehensive investigation should be carried out in order to find the limits, within which this approximation is acceptable, for practical computations.

The results obtained in the case of the computation of the safety factor of an 80-m high earth- and rockfill dam are shown on Fig. 5. In the graphical solution the active force (E_a) needed to hold the core section in equilibrium was compared to the passive resistance (E_p) of the supporting rockfill wedge for several safety factors. The safety factor of the slope, for which $E_a = E_p$, was obtained by graphical interpolation. The computation was repeated for the same slip surface using Eq 11 and assuming $\Delta T = 0$, and with a distribution of the T forces satisfying Eqs 12 and 14. It is readily seen that the results comply closely with the graphical computation.

Another case shown on Fig. 6 demonstrates the computation of the safety factor of the sea coast in a harbour. In this case the graphical computation and the numerical computation with Eq 11 again gave nearly the same results. Eq 1, however, yielded a much lower safety factor.

These examples show that the graphical computation and the numerical computation with Eqs 11, 12, and 14 are equivalent and they can be used in practice with equal justification. The great advantage of the numerical procedure is that it can be modified for use with digital computers. In complicated cases like the stability analysis of slopes of non-homogeneous dam sections the use of a computer can result in increased accuracy with substantial saving in time and labour.

REFERENCES

BISHOP, A. W. (1955). The use of the slip circle in the stability analysis of slopes. *Géotechnique*, Vol. 5, No. 1.

JANBU, N. (1954). Application of composite slip surfaces for stability analysis. *Proc. European Conference on Stability of Slopes*, Vol. 3, p. 43.

KREY, H. (1936). *Erddruck, Erdwiderstand und Tragfaehigkeit des Baugrundes* (Pressure, stability and bearing capacity of Soils). Berlin, Ernst, 348 pp.

NONVEILLER, E. (1953). The stability of slopes of nonhomogeneous dams. *Proc. Third International Conference on Soil Mechanics and Foundation Engineering*, Vol. 2.

——— (1955). Neka razmatranja o proračunu, stabilnosti nasutih brana (Certain considerations regarding the calculations of stability of fill dams), *Tehnika*, vol. 10, pp. 665–70.

——— (1957a). Discussion, *Fourth International Conference on Soil Mechanics and Foundation Engineering*, Vol. 3.

——— (1957b). *Stabilnost nehomogenih nasipa*, Beograd.

REINIUS, E. (1955). The stability of the slopes of earth dams. *Géotechnique*, Vol. 5, No. 2.

——— (1961). The stability of the downstream part of earth dams. *Bull.* No. 59, Division of Hydraulics, Royal Institute of Technology, Stockholm.

SAMSIOE, A. F. (1955). Stresses in downstream part of an earth or rock fill dam. *Géotechnique*, Vol. 5, No. 2.

TAYLOR, D. W. (1948). *Fundamentals of soil mechanics*. New York, Wiley, p. 700.

TROLLOPE, D. H. (1957). The systematic arching theory applied to the stability of dams. *Proc. Fourth International Conference on Soil Mechanics and Foundation Engineering*, Vol. 2.